J. Fluid Mech. (1974), *vol.* 64, *part* 2, *pp.* 263–287
Printed in Great Britain

Turbulent flow in smooth concentric annuli with small radius ratios

By K. REHME

Institut für Neutronenphysik und Reaktortechnik, Kernforschungszentrum, 75 Karlsruhe, Germany

(Received 25 May 1973)

Fully developed turbulent flow through three concentric annuli was investigated experimentally for a Reynolds-number range $Re = 2 \times 10^4$–2×10^5. Measurements were made of the pressure drop, the positions of zero shear stress and maximum velocity, and the velocity distribution in annuli of radius ratios $\alpha = 0{\cdot}02$, $0{\cdot}04$ and $0{\cdot}1$, respectively. The results for the key problem in the flow through annuli, the position of zero shear stress, showed that this position is not coincident with the position of maximum velocity. Furthermore, the investigation showed the strong influence of spacers on the velocity and shear-stress distributions. The numerous theoretical and experimental results in the literature which are based on the coincidence of the positions of zero shear stress and maximum velocity are not in agreement with reality.

1. Introduction

Fully developed turbulent flow in smooth concentric annuli has been studied in many experiments and numerous theoretical investigations. Despite the fact that there are so many results there is no general agreement on the interpretation of such basic quantities as the pressure-drop coefficient and velocity profiles. The key problem in the flow through concentric annuli is the determination of the position of zero shear stress and hence, the wall shear stresses at the inner and outer walls, respectively. Up to now, the coincidence of zero shear stress and maximum velocity has been assumed in nearly all investigations.

Yet, this assumption does not hold in the case of asymmetric velocity profiles, as has been shown earlier (Kjellström & Hedberg 1966; Maubach & Rehme 1972). The annulus is the simplest geometry with smooth walls to generate an asymmetric velocity profile. Certainly this is the reason for the numerous experimental and theoretical investigations, which will be summarized briefly below.

1.1. *Experimental investigations*

In the early papers by Knudsen & Katz (1950, 1958) and Rothfus and coworkers (Rothfus 1948; Rothfus, Monrad & Senecal 1950; Rothfus *et al.* 1955) it was assumed that the positions of zero shear stress and maximum velocity were coincident as in the case of laminar flow, although the experimental results of Lorenz (1932) had clearly shown that in turbulent flow the position of maximum velocity was nearer to the inner wall than in laminar flow. The same result was reported by Koch & Feind (1958) and Nicol & Medwell (1964). Leung, Kays & Reynolds (1962) and Kays & Leung (1963) were the first authors to establish a formula for the position of the maximum velocity of turbulent flow; this position, which depends on the radius ratio, is assumed to be independent of the Reynolds number:

$$\frac{\hat{r}-r_1}{r_2-\hat{r}} = \left(\frac{r_1}{r_2}\right)^{0.343}, \tag{1}$$

r_1 and r_2 being the inner and outer radius, respectively, and $\hat{r}$ the radius of maximum velocity.

This relation has been verified by many authors in subsequent years (Brighton 1963; Brighton & Jones 1964; Okiishi & Serovy 1964; Y. Lee 1964; Jonsson 1965; Jonsson & Sparrow 1966; Sartory 1962; Rothfus, Sartory & Kermode 1966; Ivey 1965; Ball & Azer 1972). The most important experimental investigation is that by Brighton (1963). The results of his study served as the basis of numerous models for calculation of turbulent flow in annuli.

Brighton very carefully measured the velocity profiles and the position of the maximum velocity by means of a double Pitot tube. Besides, he was the first author also to measure turbulence intensities and shear-stress distributions by means of hot wires. From his measurements of the shear-stress distributions Brighton concluded that the positions of zero shear stress and maximum velocity were identical. However, the scatter of the experimental data on the shear-stress distribution was so great that this conclusion was not warranted by his measurements.

Kjellström & Hedberg (1966), in their fundamental work, for the first time explained that zero shear stress and maximum velocity need not necessarily occur in the same place except in cases in which this is required for reasons of symmetry (circular tubes or parallel plates). They verified the non-coincidence in the case of annuli with rough inner tubes. Kjellström & Hedberg also measured the shear-stress distribution and the velocity profiles in a smooth annulus. In this case, they found coincidence of the positions because they chose a radius ratio of $\alpha = r_1/r_2 = 0.446$; the velocity profile was only slightly asymmetric and the difference in the positions was within the limits of experimental error.

Quarmby (1967*b*, 1968*a*) showed experimentally that the position of maximum velocity cannot be determined very precisely by means of Pitot tubes or double Pitot tubes. In order to identify this position, which he believes to be coincident with the position of zero shear stress, more accurately, Quarmby used the Preston-tube method (Preston 1954) to determine the wall shear stresses at the inner and outer walls, respectively. The Preston-tube method was also employed by Barthels (1967), although the validity of universal laws of velocity must be supposed, a condition which has not been justified, despite the investigation of Quarmby (1967*a*), as Eifler (1970) showed.

Smith, Lawn & Hamlin (1968) developed a new method, the 'sliding sleeve' method, to measure the wall shear stress at the inner wall directly. The results of their measurements and of further measurements by Lawn & Elliott (1971, 1972) for the first time showed that the positions of zero shear stress and maximum velocity are non-coincident even in the case of smooth annuli. Lawn & Elliott used the hot-wire technique to measure the shear-stress distribution; the 'sliding sleeve' method was used only for comparison. Lawn & Elliott concluded from their studies that zero shear stress occurred closer to the inner surface than the maximum velocity, the positions of zero shear stress were in excellent agreement with the Kays–Leung equation and that there were considerable deviations from universal laws for the velocity profiles of the inner zone. The core tubes in the investigations of Lawn & Elliott were kept in a concentric position by 'several' spacers each consisting of three wires. The influence of such spacers on the velocity and turbulence distributions will be discussed below.

1.2. *Theoretical investigations*

Of course, numerous attempts have been made to describe the experimental velocity profiles theoretically. Rothfus, Walker & Whan (1958) obtained velocity profiles in circular tubes, like those developed by Nikuradse (1932), also for annuli by modifying the co-ordinate normal to the wall. Barrow, Lee & Roberts (1965) offered a modification of the constants κ and B of the law of the wall

$$u^+ = \kappa^{-1} \ln y^+ + B \tag{2}$$

in the inner zone for 'engineering purposes'. Their method gives positions of maximum velocity closer to the laminar solution than the Kays–Leung equation.

After Brighton's results were published, a number of theoretical papers involving different methods closely followed these experimental results. Ratkowsky (1966) extended the equations of Rothfus *et al.*; Levy (1967), Roberts (1967), Michiyoshi & Nakajima (1968) and Gräber (1970) calculated the position of maximum velocity using the Kays–Leung equation. Clump & Kwasnoski (1968), Eifler (1968, 1969) and Min, Hoffman & Peebles (1971) performed their calculations by modifying the constants of the law of the wall through an evaluation of the experimental results of Brighton.

Universal laws of the velocity distribution in circular tubes were applied to annuli by Tiedt (1966, 1967, 1968), Macagno & McDougall (1966), Maubach (1969, 1970) and Wilson & Medwell (1968) and further improved by Quarmby (1968) and Quarmby & Anand (1970). The results of these authors show that the position of the maximum velocity, which is taken as the zero-shear-stress position, is nearer to the inner surface than it is according to the Kays–Leung equation. Velocity profiles in annuli were also calculated by Patel (1973) using an advanced 'mixed-length' model. The theoretical and experimental investigations by Rao (Rao & Keshavan 1972) on axisymmetric boundary layers on circular cylinders are also relevant to the flow through annuli especially for small radius ratios.

The survey of different experimental and theoretical results from the literature indicates that the following steps should be taken: (i) determine the position of zero shear stress very carefully by a direct method; (ii) check whether there are deviations from the velocity profiles in tubes for radius ratios $\alpha < 0{\cdot}1$ due to the asymmetry present in this case; (iii) get sufficient and reliable experimental results for radius ratios $\alpha < 0{\cdot}1$.

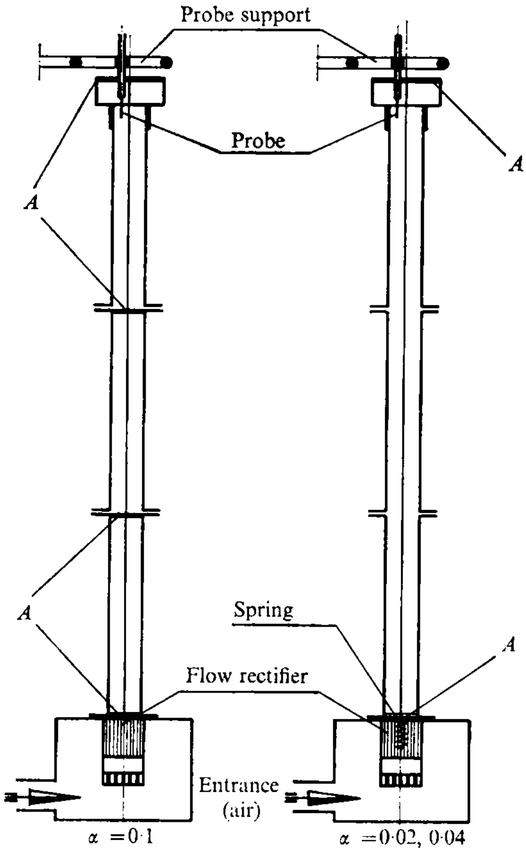

FIGURE 1. Test section (schematic). *A*, spacer.

2. Experimental apparatus

Experiments were performed using an open air rig with annuli of three radius ratios $\alpha = 0{\cdot}02$, $0{\cdot}04$ and $0{\cdot}1$, respectively, for a range of Reynolds numbers between $Re = 2 \times 10^4$ and $Re = 2 \times 10^5$. The pressure drop and shear-stress and velocity distributions were investigated.

The air rig and the outer brass tube (I.D. 99·97 mm, length 7500 mm) were those used earlier (Rehme 1972*a*). The cores consisted of a stainless-steel rod of diameter 9·98 mm in the case $\alpha = 0{\cdot}1$ and of aluminium wires of diameters 3·96 and 1·98 mm in the cases $\alpha = 0{\cdot}04$ and $\alpha = 0{\cdot}02$, respectively, resulting in ratios of length to hydraulic diameter of 83·3, 78·1 and 76·5, respectively. The concentric position was achieved using spacers at the inlet and outlet and, in the case $\alpha = 0{\cdot}1$, two other spacers. The wires were stretched and tensioned by a spring (see figure 1).

With the annuli with $\alpha = 0{\cdot}04$ and $0{\cdot}02$, respectively, spacers were avoided because measurements with the $\alpha = 0{\cdot}1$ annulus showed that the velocity and turbulence distributions were not completely established 27·8 hydraulic diameters downstream of the spacer. To minimize disturbances to the flow, spacers with three radial struts were used first. Measurements of the velocity and turbulence distributions on two perpendicular radii showed considerable deviations.

Further measurements with the spacer rotated showed that the positions of zero shear stress and the velocity distribution varied with the spacer orientation. Different orientations of the spacer caused differences of up to 1·5 mm between the measured positions of zero shear stress at constant Reynolds number, whereas the measured positions of zero shear stress at constant geometry were reproduced to within $\pm 0{\cdot}1$ mm. The velocity distributions on different radii showed differences of up to 3 % at the same radial position, whereas the maximum difference was 0·8 % in the cases without spacers.

As it was impossible in the case of the 10 mm rod to run the experiment without supports, new spacers with four radial struts were used to generate equal velocity and turbulence distributions on perpendicular radii for symmetry reasons. Of course the disturbances to the flow caused by the spacers were not overcome in this way.

The mass flow rate was measured by means of an orifice plate. The velocity distributions were measured by means of Pitot tubes (0·6 mm outer diameter), the turbulence distributions by a DISA hot-wire anemometer. For comparison, the wall shear stresses were determined by Preston tubes using the Patel (1965) calibration. For details, see Rehme (1972*a*).

3. Results and discussion

3.1. *Bases of evaluation*

All results were computed on an IBM 360/165. The time-mean velocity $\overline{u}$ was calculated from Pitot-tube measurements as

$$\overline{u} = (2\Delta p/\rho_h)^{\frac{1}{2}}, \tag{3}$$

with Δp the differential pressure and ρ_h the density of humid air. The velocity measurements were corrected for the influence of the wall according to MacMillan (1956) and for the influence of the turbulence intensities according to an equation of Eifler (1970) based on the measurements of Laufer (1954) in circular tubes.

For evaluation of the hot-wire measurements a method developed by Kjellström & Hedberg (1968, 1970) and tested by Durst, Melling & Whitelaw (1971) was adopted.

The pressure-drop coefficient λ is defined by

$$\lambda = \frac{\Delta p/\Delta L}{\frac{1}{2}\rho_h\,\overline{u}_m^2/d_h}, \tag{4}$$

with the hydraulic diameter $d_h = 2(r_2-r_1)$, and the Reynolds number can be calculated from

$$Re = \rho_h\,\overline{u}_m d_h/\eta, \tag{5}$$

where $\overline{u}_m$ is the fluid velocity averaged over the cross-section, calculated on the basis of the measured mass flow rate, d_h is the hydraulic diameter and η the dynamic viscosity.

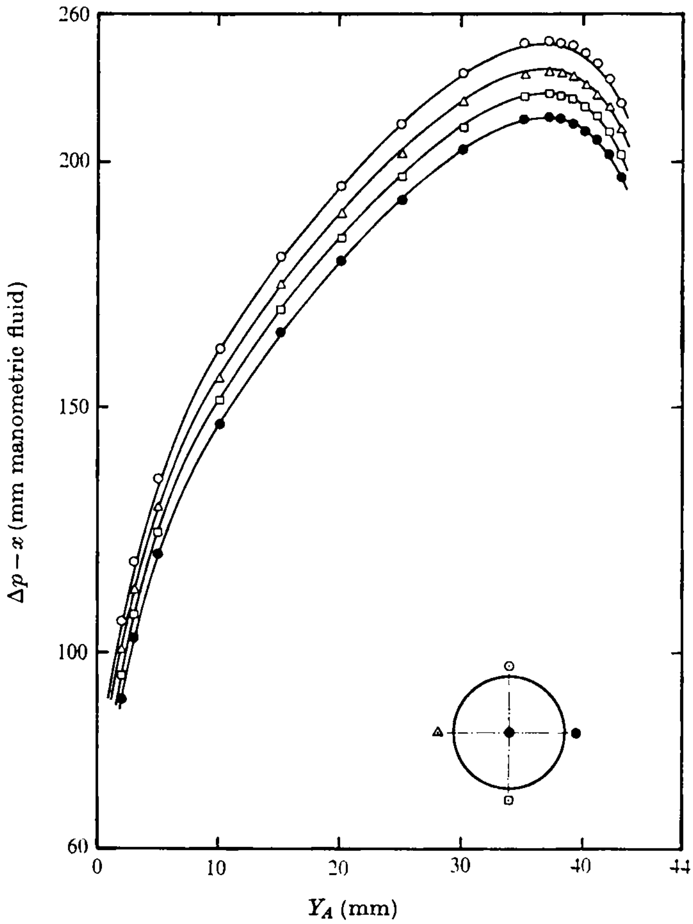

FIGURE 2. Symmetry of velocity distribution. $\alpha = 0{\cdot}0396$, $Re = 1{\cdot}99 \times 10^5$. Inset shows radii along which measurements were taken. ○, $x = 0$; △, $x = 5$ mm; □, $x = 10$ mm; ●, $x = 15$ mm; ——, average of four runs; Y_A measured from outer wall.

3.2 *Symmetry of the velocity profile*

It was assumed that the flow was fully developed, because the length-to-diameter ratios were higher than 76. To test whether the flow was symmetric, velocity profiles were measured on four radii located at right angles to each other. As an example, figure 2 shows the results for the radius ratio $\alpha = 0{\cdot}04$. The symmetry of the flow is excellent. The maximum deviation from the mean value is 0·8 %, i.e. the velocities on the same radius agree to within $\pm 0{\cdot}4$ %.

3.3. *Pressure drop*

The pressure drop for the flow through the three annuli was measured over a length $L = 2106$ mm. The pressure-drop coefficients evaluated from these measurements are plotted in figure 3 as a function of the Reynolds number.

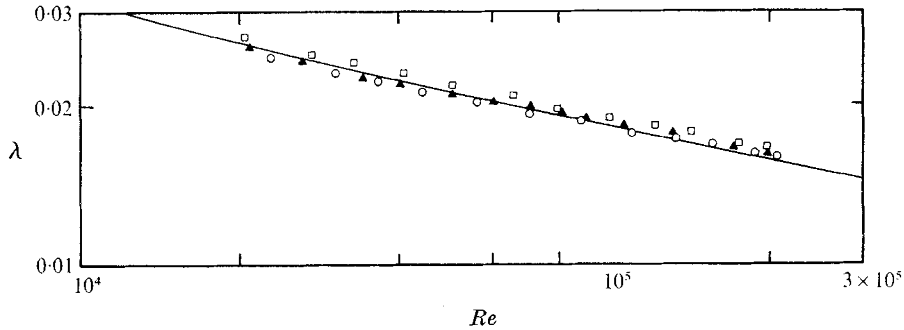

FIGURE 3. Pressure-drop coefficient *vs.* Reynolds number. ○, $\alpha = 0{\cdot}02$; ▲, $\alpha = 0{\cdot}04$; □, $\alpha = 0{\cdot}1$; ——, circular tube, $\lambda^{-\frac{1}{2}} = 2{\cdot}035 \log_{10}(Re\,\lambda^{\frac{1}{2}}) - 0{\cdot}989$.

For comparison, the pressure-drop law for circular tubes as given by Maubach (1970) has been added:

$$\lambda^{-\frac{1}{2}} = 2{\cdot}035 \log_{10}(Re\,\lambda^{\frac{1}{2}}) - 0{\cdot}989. \tag{6}$$

The following conclusions can be drawn.

(i) The pressure-drop coefficients increase slightly with increasing radius ratio. This is in excellent agreement with the theoretical dependence obtained by Eifler (1968), Tiedt (1966, 1967, 1968), Maubach (1969) and Quarmby (1968*b*). For a Reynolds number $Re \approx 10^5$ and a radius ratio $\alpha = 0{\cdot}02$ the experimental pressure-drop coefficients coincide with the circular-tube values; for $\alpha = 0{\cdot}04$ they are about 1·1 % and for $\alpha = 0{\cdot}1$ about 4 % higher than the circular-tube values. It is interesting to note that the dependence of the pressure-drop coefficients on the Reynolds number in the cases $\alpha = 0{\cdot}04$ and $\alpha = 0{\cdot}02$, respectively, is slightly different from that for a tube. This may be due to the fact that the flow is still in a transition region in the case of the two lower radius ratios investigated.

(ii) The conclusion drawn by Lawn & Elliott (1971, 1972) according to which the pressure-drop coefficients of parallel plates are about 5 % higher than the circular-tube values obviously proves to be true, especially in the light of theoretical results. The further conclusion of Lawn & Elliott, that with increasing radius ratio this upper limit is reached from higher values, is proved to be wrong by the new measurements.

(iii) The dependence on radius ratio of the pressure-drop coefficient with a maximum value for $\alpha = 0{\cdot}6$ as elaborated by Barthels (1967) obviously is as incorrect as the dependence given by Davis (1943), who came to the conclusion that the friction factor decreases with increasing radius ratio. The experimental results recently published by Ball & Azer (1972), which are up to 30 % above the circular-tube values, undoubtedly are wrong for smooth annuli.

In the further evaluation of the data the following pressure-drop laws were used:

$$\lambda^{-\frac{1}{2}} = 1{\cdot}9505 \log_{10}(Re\,\lambda^{\frac{1}{2}}) - 0{\cdot}80581 \quad \text{for} \quad \alpha = 0{\cdot}1, \tag{7}$$

$$\lambda^{-\frac{1}{2}} = 1{\cdot}9177 \log_{10}(Re\,\lambda^{\frac{1}{2}}) - 0{\cdot}58007 \quad \text{for} \quad \alpha = 0{\cdot}04, \tag{8}$$

$$\lambda^{-\frac{1}{2}} = 1{\cdot}8354 \log_{10}(Re\,\lambda^{\frac{1}{2}}) - 0{\cdot}16802 \quad \text{for} \quad \alpha = 0{\cdot}02. \tag{9}$$

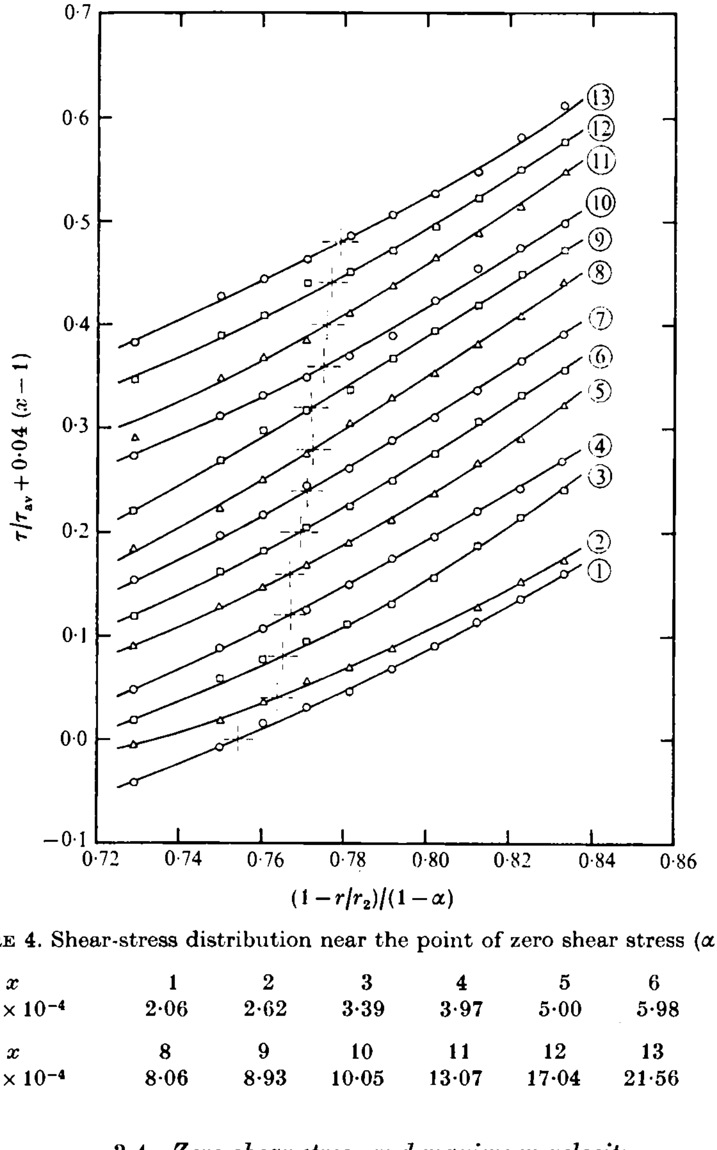

FIGURE 4. Shear-stress distribution near the point of zero shear stress (α = 0·04).

x	1	2	3	4	5	6	7
$Re \times 10^{-4}$	2·06	2·62	3·39	3·97	5·00	5·98	7·04
x	8	9	10	11	12	13	
$Re \times 10^{-4}$	8·06	8·93	10·05	13·07	17·04	21·56	

3.4. *Zero shear stress and maximum velocity*

To determine the positions r_0 of zero shear stress, the shear-stress distributions evaluated from the hot-wire measurements were plotted against distance across the gap.

Figure 4 is an example of such a plot. Since the scatter of the experimental data is small, the positions of zero shear stress were determined quite accurately. The radius of zero shear stress was determined with an accuracy of $\pm$ 0·05 mm from the experimental data. An interval of 0·01 on the abscissa in figure 4 corresponds to 0·48 mm.

The same procedure was adopted to determine the maximum velocity. In this case, the differential pressures measured by the double Pitot tube yielded

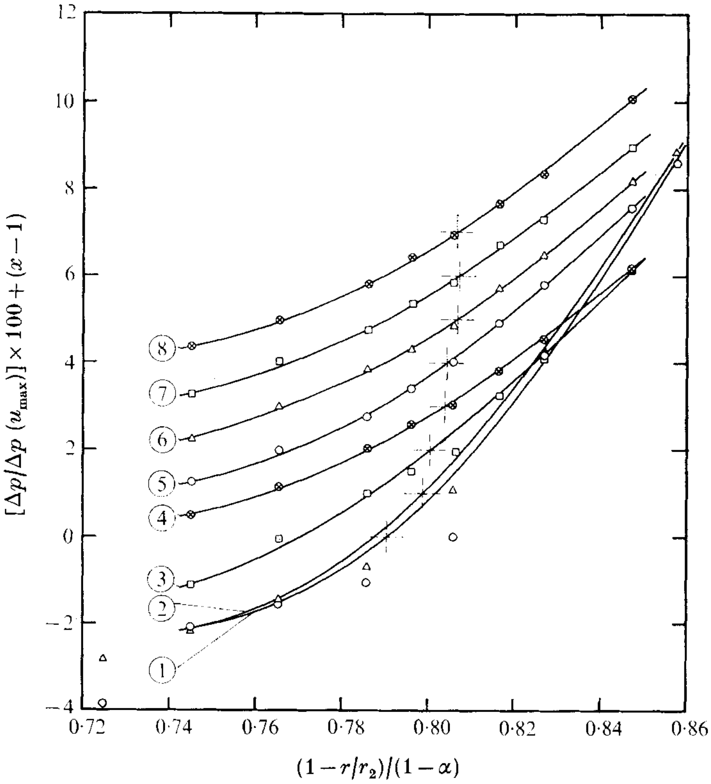

FIGURE 5. Distribution of velocity gradient in the region of maximum velocity (α = 0·02).

x	1	2	3	4	5	6	7	8
$Re \times 10^{-4}$	4·41	5·62	8·87	11·81	13·24	16·09	18·88	20·57

the maximum-velocity locus. As can be seen from figure 5, the accuracy is very bad for $Re < 10^5$. This is because the differential pressures become very small and thus the measurements are not very precise. The curves were drawn through the scattered data by taking into account the outer points only, which are believed to be more precise because the differential pressures are higher. Quarmby (1968*a*) has called attention to this point before. Another disadvantage of measurements with a double Pitot tube in the case of extremely asymmetric velocity profiles lies in the fact that the measured value cannot be assumed to be the actual velocity halfway between the two Pitot tubes. The fluid velocities at a certain distance either side of the maximum are not equal. In this case of smooth annuli, the velocity in the inner zone is lower than in the outer zone, thus causing the measured position of the maximum velocity to be too far away from the inner wall.

The results for the positions of zero shear stress $\beta = r_0/r_2$ and maximum velocity $\hat{\beta} = \hat{r}/r_2$ are plotted against the Reynolds number in figure 6 for the different radius ratios. For comparison with the different theoretical expressions, the values calculated by Kays & Leung (1963), by Eifler (1969) and by Maubach (1969) have been added to the figures.

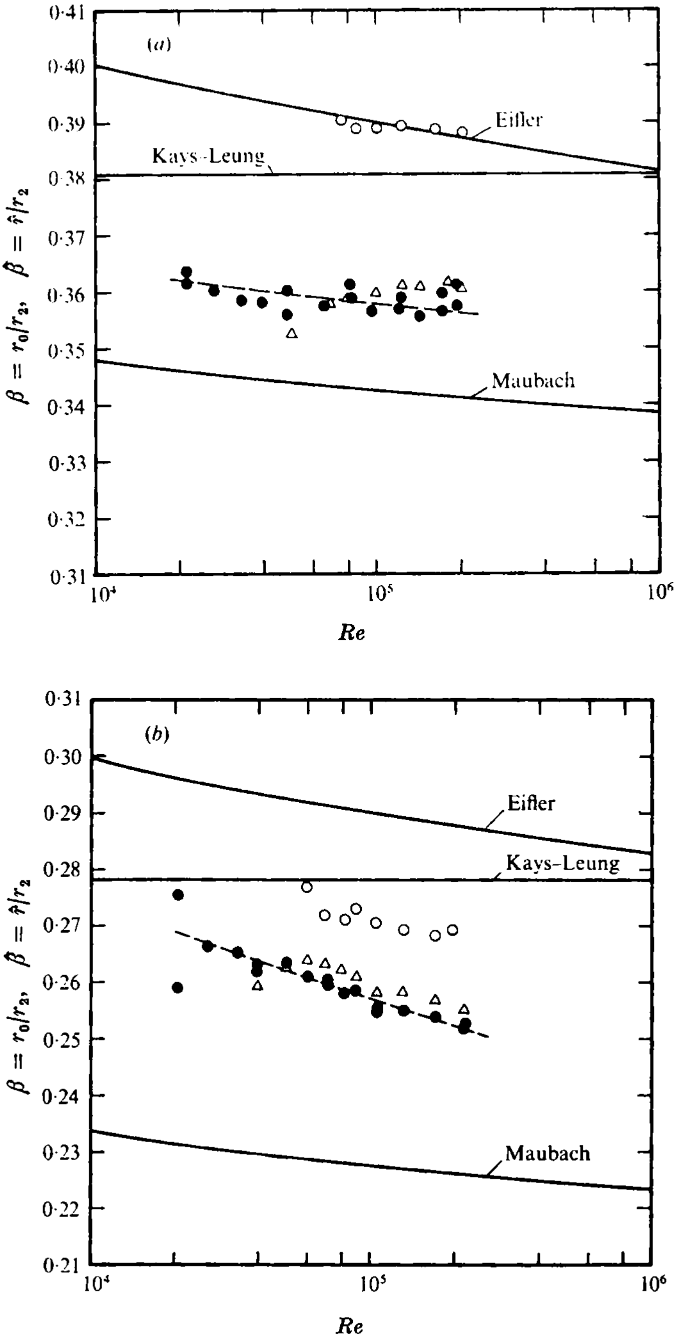

FIGURES 6 (a, b). For legend see facing page.

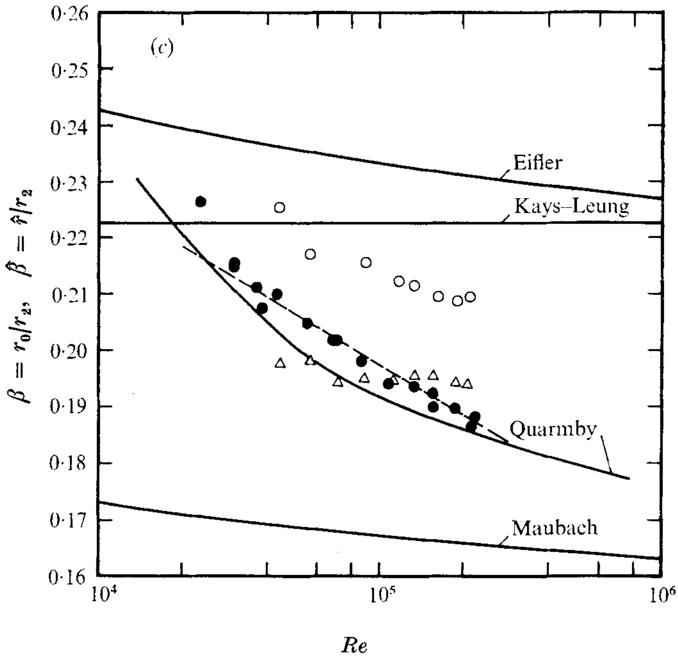

FIGURE 6. Experimental values of the positions at zero shear stress and maximum velocity, respectively, *vs.* Reynolds number. ●, hot wire, $\tau = 0$; △, Preston tube, $\tau = 0$; ○, double Pitot tube, u_{max}. (*a*) $\alpha = 0{\cdot}10$. (*b*) $\alpha = 0{\cdot}04$. (*c*) $\alpha = 0{\cdot}02$.

All the radius ratios investigated can be characterized by the following statements.

(i) The positions of zero shear stress and maximum velocity are non-coincident, as was supposed for asymmetric velocity profiles (Maubach & Rehme 1972). The position of zero shear stress in every case is distinctly closer to the inner tube than the position of maximum velocity.

(ii) The measured positions of zero shear stress deviate from the positions predicted by Kays & Leung, Eifler and Maubach. The experimental data are not as close to the inner surface as had been calculated by Maubach. Maubach finds this position to be at the intersection of the two velocity profiles starting from the walls, which are assumed to be laws of the wall (Nikuradse). On the other hand, the experimental data are closer to the inner surface than has been calculated by Eifler or predicted by Kays & Leung. The expression found by Kays & Leung was elaborated empirically on the basis of measurements of the maximum velocity by various authors, especially the data of Lorenz for a radius ratio $\alpha = 0{\cdot}0526$. However, both Eifler and Maubach calculated the intersection of the two velocity profiles, but Eifler, in contrast to Maubach, used velocity profiles generated by adjustment of the constants to the experimental data of Brighton.

(iii) The positions of zero shear stress calculated from the experimental wall shear stresses at the inner and outer surfaces measured by Preston tubes are in excellent agreement with the hot-wire results. At low Reynolds numbers these measurements become inaccurate because of the very low differential pressures.

In particular the following facts can be established.

(i) $\alpha = 0{\cdot}1$. The experimental data for the zero-shear-stress position are only weakly dependent on the Reynolds number (see figure 6*a*). The positions measured for the maximum velocity are in excellent agreement with the calculations by Eifler. The measured values indicate a large difference between the positions of maximum velocity and zero shear stress. These findings can be explained only by the flow disturbances caused by the spacers. The measurements with the double Pitot tube were not performed initially, but had to be made after the measurements with the radius ratios $\alpha = 0{\cdot}02$ and $\alpha = 0{\cdot}04$. This, of course, necessitated reconstruction of the test section, which may have caused deviations of the geometry, especially of the spacer orientation, compared with that for the shear-stress measurements. Further investigations of this point were given up because the measurements for the radius ratio $\alpha = 0{\cdot}1$ are not as significant as the measurements for $\alpha = 0{\cdot}02$ and $\alpha = 0{\cdot}04$, because of the evident influences on the flow distribution of the spacers.

(ii) $\alpha = 0{\cdot}04$. In this case (see figure 6*b*), the positions of maximum velocity and zero shear stress do not coincide, but the difference between them is smaller than in the case $\alpha = 0{\cdot}1$. At a Reynolds number $Re \approx 10^5$ the difference between the positions was $\Delta = 1{\cdot}6$ mm for $\alpha = 0{\cdot}1$, i.e. relative to the inner profile length $l = 12{\cdot}8$ mm it was $12{\cdot}5$ %. For the radius ratio $\alpha = 0{\cdot}04$ we found that $\Delta = 0{\cdot}8$ mm and with $l_1 = 10{\cdot}6$ mm, a relative deviation of $7{\cdot}5$ %. The dependence on the Reynolds number of the positions is similar for both positions and stronger than the dependence calculated by Eifler and Maubach, respectively.

(iii) $\alpha = 0{\cdot}02$. The dependence of the positions of zero shear stress and maximum velocity on the Reynolds number is even more pronounced for the radius ratio $\alpha = 0{\cdot}02$ (see figure 6*c*). The positions differ by about $1{\cdot}0$ mm, which results in a relative difference of 12 % with a profile length of $l_1 = 8{\cdot}4$ mm. Compared with the case $\alpha = 0{\cdot}04$, the relative difference increases, as is to be expected owing to the higher level of asymmetry.

The results of another theoretical paper have been added to figure 6(*c*). Quarmby (1968*b*) computed the position of maximum velocity (zero shear stress) as the point of intersection of the two velocity profiles. In contrast to both Eifler and Maubach, his velocity profiles were calculated by integration of differential equations by means of a Runge–Kutta technique.

Quarmby (1969) used the same differential equations for the velocity profile as he had developed for circular tubes and parallel plates. He employed a two-zone model. For the region close to the wall the velocity profile was deduced from Deissler's (1955) expression for the eddy diffusivity in the sublayer. The velocity profile outside the sublayer was deduced from an expression due to J. Lee (1965) based on the extension of the von Kármán similarity hypothesis by Goldstein (1938).

The curve in figure 6(*c*) calculated by Quarmby (1968*b*) is an excellent description of the measured zero-shear-stress position. This proves also that

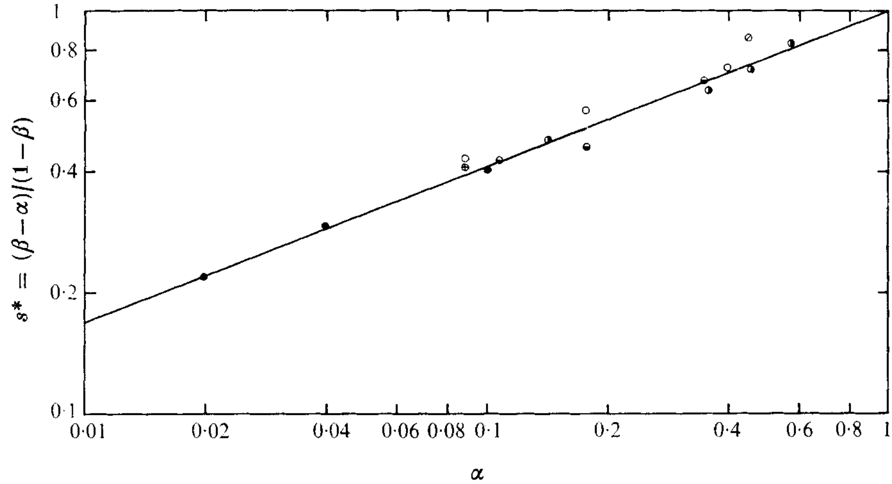

FIGURE 7. Experimental values of the position of zero shear stress *vs.* radius ratio. $Re = 10^5$. ⊗, Smith *et al.*; ⊖, Quarmby; ◑, Barthels; ⊘, Kjellström & Hedberg; ○, Lawn & Elliott; ●, present results.

flows with strongly asymmetric velocity profiles and widely differing wall curvatures are described sufficiently well by the circular-tube findings.

Simpler expressions for the velocity profile, however, such as the law of the wall of Nikuradse, are insufficient, at least for low Reynolds numbers. The zero-shear-stress positions for higher Reynolds numbers clearly show a tendency to approach the curve calculated from the point of intersection of the two laws of the wall (Maubach).

Of course, the Quarmby method is unable to describe special effects in the flow, such as the non-coincidence of maximum velocity and zero shear stress. However, the position of maximum velocity is of no great interest, if the position of zero shear stress can be determined with the necessary precision.

The dependence of the position of zero shear stress on the radius ratio is plotted in figure 7. For low Reynolds numbers this position is strongly dependent on the Reynolds number; therefore, in figure 7 only the values for a Reynolds number of $Re \approx 10^5$ are used. In accordance with Kays & Leung, the ordinate variable is chosen as

$$s^* = (\beta-\alpha)/(1-\beta). \tag{10}$$

According to Kays & Leung, we get

$$s^* = \alpha^n, \tag{11}$$

with $n = 0{\cdot}343$. Quarmby (1967*b*), on the basis of his experimental results, found $n = 0{\cdot}366$; theoretically, from his analysis (Quarmby 1968*b*), he obtained $n = 0{\cdot}415$, for high Reynolds numbers only. In the figure, only those experimental results are plotted which were obtained either from hot-wire measurements (Smith *et al.* 1968; Kjellström & Hedberg 1966; Lawn & Elliott 1971; present results) or Preston-tube measurements (Barthels 1967; Quarmby 1967*b*),

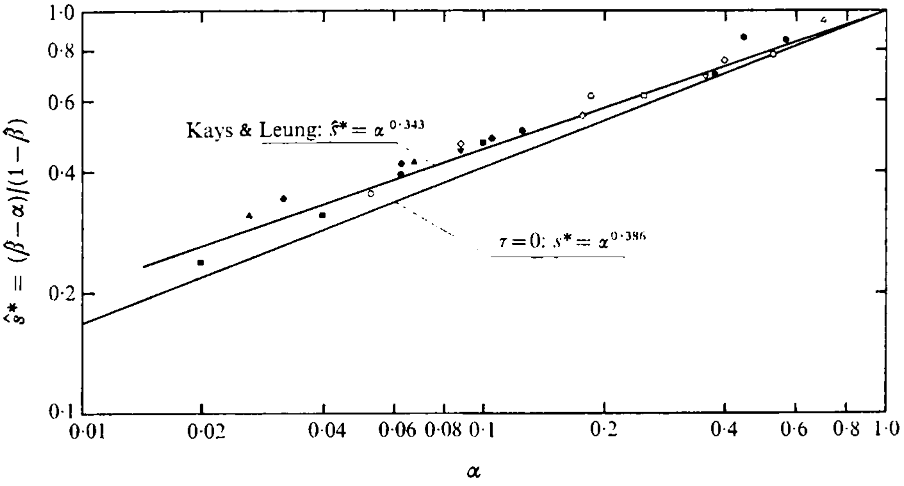

FIGURE 8. Experimental values of the position of maximum velocity *vs.* radius ratio. $Re = 10^5$. ○, Lorenz; △, Nicol & Medwell; ▲, Sartory; □, Ball & Azer; ⊗, Kjellström & Hedberg; ▼, Smith *et al.* Measurements using double Pitot tube: ●, Brighton; ▽, Quarmby; ◇, Lawn & Elliott; ◆, Crookston and Crookston *et al.*; ■, present results.

since the zero-shear-stress position is determined by these methods and the results of both methods agree very well, as we saw above.

If the new measured results are considered, since they were obtained for low radius ratios and without spacers, the exponent in (11) is found to be $n = 0{\cdot}386$ for a Reynolds number $Re \approx 10^5$. This value is higher than Quarmby's experimental value, but lower than his theoretical value, since a high Reynolds number was supposed in the latter case.

For comparison, numerous results in the literature concerning the position of maximum velocity, are plotted with our results in figure 8. Besides the values referred to in the survey of the literature, the experimental results of Crookston (Crookston 1966; Crookston, Rothfus & Kermode 1968) are shown for radius ratios $\alpha = 0{\cdot}0318$, $0{\cdot}0627$ and $0{\cdot}1047$, respectively. The experimental results are fitted quite well by the Kays–Leung relation ($n = 0{\cdot}343$), the line of the zero shear stress ($n = 0{\cdot}386$) being definitely lower than the line for the maximum velocity. The results of Sartory for $\alpha = 0{\cdot}0262$ and of Crookston for $\alpha = 0{\cdot}0318$ are higher than the new measured results for $\alpha = 0{\cdot}02$ and $\alpha = 0{\cdot}04$. This is believed to be due to the influence of the sag of the wires in the horizontal test sections used by Crookston and by Sartory. Crookston used additional spacers, which, however, prevent the development of the flow and cause disturbances of the velocity profile, as has been shown.

For further evaluation, especially for the dimensionless velocity profiles, the position of zero shear stress was calculated using the following relations, which correspond to the broken lines in figure 6:

$$\beta = 0{\cdot}3864 - 0{\cdot}0057 \log_{10} Re \quad \text{for} \quad \alpha = 0{\cdot}1, \tag{12}$$

$$\beta = 0{\cdot}342 - 0{\cdot}017 \log_{10} Re \quad \text{for} \quad \alpha = 0{\cdot}04, \tag{13}$$

$$\beta = 0{\cdot}345 - 0{\cdot}02955 \log_{10} Re \quad \text{for} \quad \alpha = 0{\cdot}02. \tag{14}$$

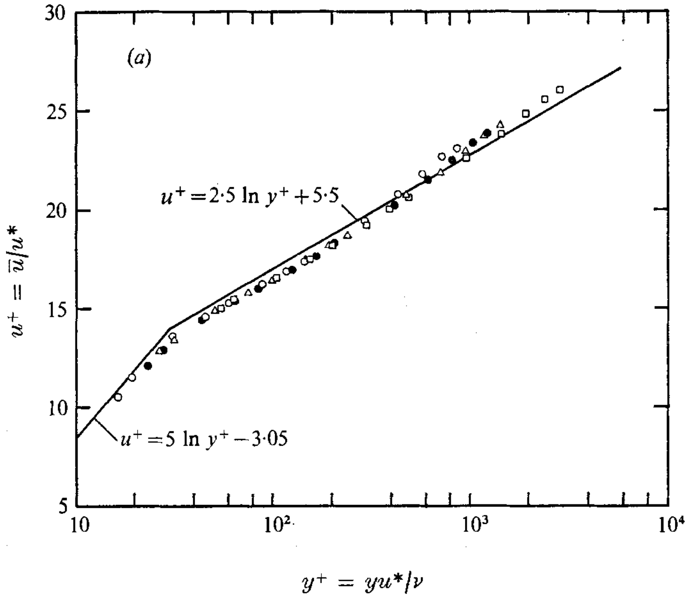

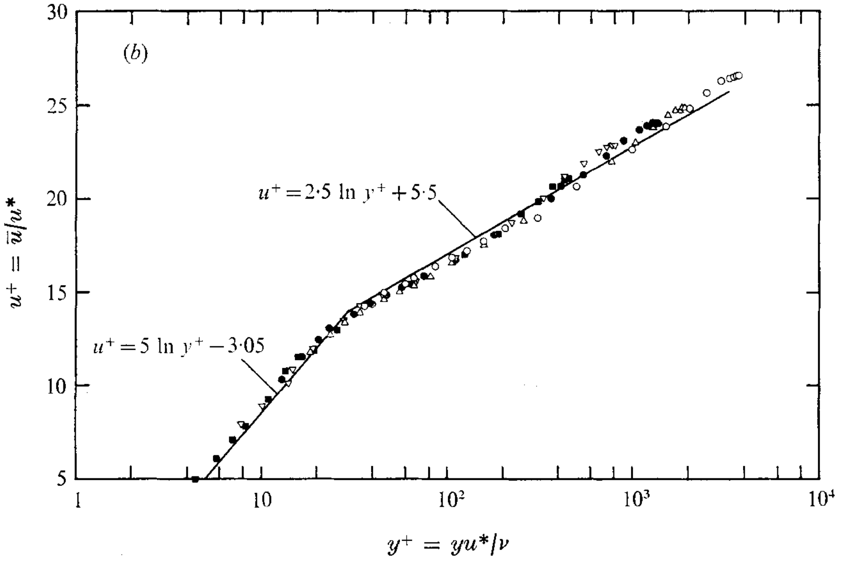

FIGURES 9(a, b). For legend see next page.

3.5. *Velocity profiles*

Outer zone. The experimental results for the velocity profiles in the outer zone are plotted in figure 9 for the three radius ratios investigated. For comparison of the results, two straight orientation lines are added; for the region $5 < y^+ < 30$

$$u^+ = 5 \ln y^+ - 3{\cdot}05, \tag{15}$$

according to Knudsen & Katz (1958), and in the region $y^+ > 30$

$$u^+ = 2{\cdot}5 \ln y^+ + 5{\cdot}5, \tag{16}$$

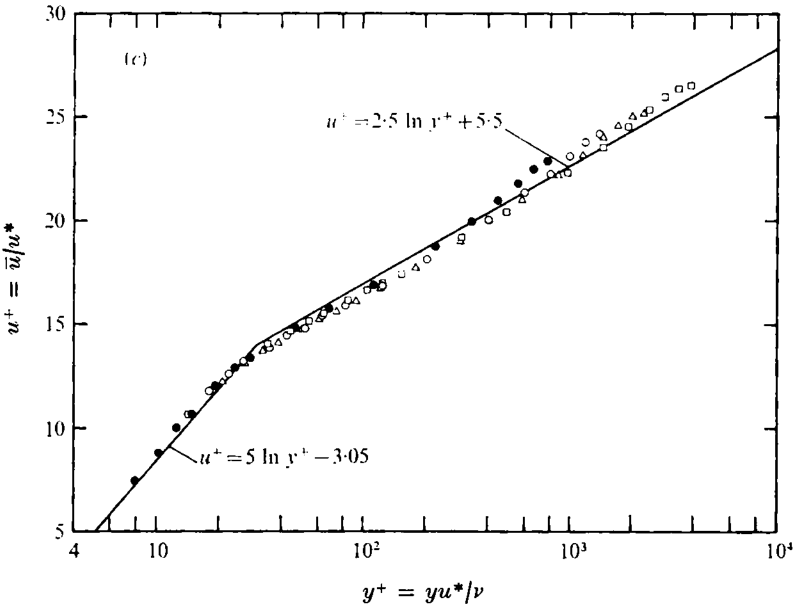

FIGURE 9. Experimental dimensionless velocity profiles in outer zone. (*a*) $\alpha = 0{\cdot}1$. (*b*) $\alpha = 0{\cdot}04$. (*c*) $\alpha = 0{\cdot}02$.

	○	●	▽	□	
(*a*) $Re \times 10^{-4}$	5·08	7·03	8·82	19·43	
	■	▽	●	△	○
(*b*) $Re \times 10^{-4}$	2·08	4·00	6·96	10·33	21·62
	●	○	△	□	
(*c*) $Re \times 10^{-4}$	4·07	7·89	11·90	20·93	

the well-known law of the wall of Nikuradse. The experimental results for all radius ratios are in excellent agreement.

Inner zone. The corresponding velocity profiles for the inner zones are plotted in figure 10. In the case $\alpha = 0{\cdot}1$, the velocity profile is fitted by the law of the wall. For the radius ratios $\alpha = 0{\cdot}04$ and $\alpha = 0{\cdot}02$, respectively, major deviations from the law of the wall can be detected. For higher Reynolds numbers, obviously the profiles are fitted by the law of the wall for a larger region. The same tendency has been discussed for the position of zero shear stress.

Comparison with the literature. A comparison with data from the literature is performed only for the inner zone of annuli, since the behaviour of the velocity profiles in the outer zone is quite similar to that in circular tubes. Differences between the positions of maximum velocity and zero shear stress have but a slight effect on the velocity profiles in the outer zones, since these zones are very large.

Figure 11(*a*) shows measurements by Brighton (1963) for a radius ratio $\alpha = 0{\cdot}0625$. Both the original data and the corrected data are plotted. The original data were corrected twice; first, the data were corrected for wall influences according to MacMillan (1956) and then, for the position of zero shear

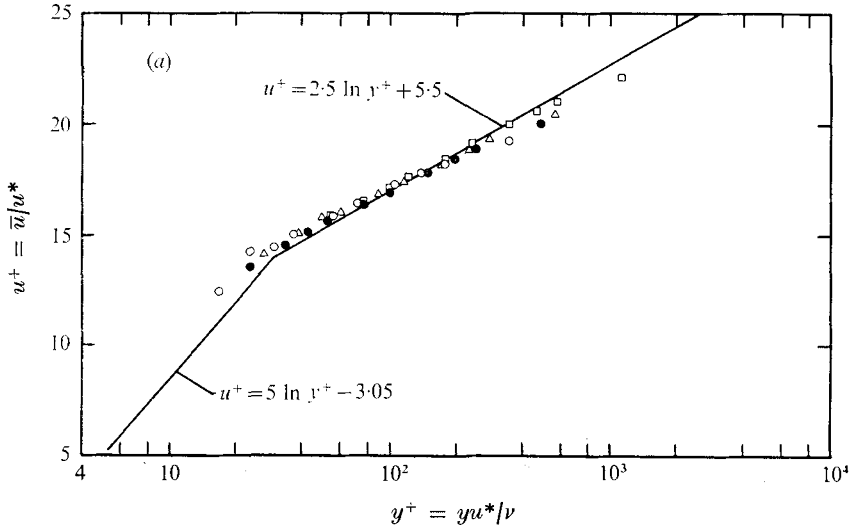

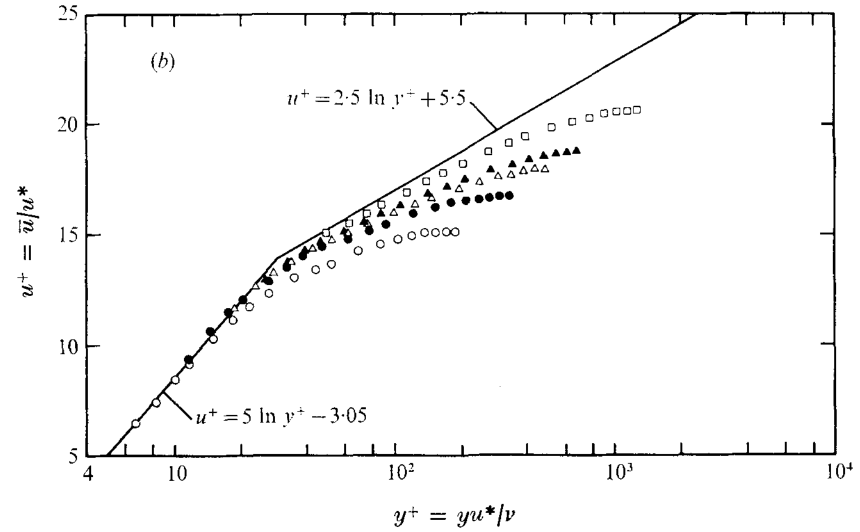

FIGURES 10 (a, b). For legend see next page.

stress according to figure 7. These corrections shift the original data some 10 % towards the law of the wall; the shifted data behave like the results of this investigation. The corrections to Brighton's data for the radius ratio $\alpha = 0{\cdot}125$ affect the original data in the same sense (see figure 11 b).

Figure 12 shows the original and the shifted data of Lawn & Elliott. They were corrected for the position of zero shear only, since the MacMillan correction had already been performed. The shifted data are 6–7 % higher than the original data, which had also been shifted in the direction of the law of the wall.

A comparison of the experimental data with theoretical predictions is shown in figures 13 and 14. The calculations by Eifler (1969) based on the data by Brighton show a deviation of 15–25 %. On the other hand, the deviations

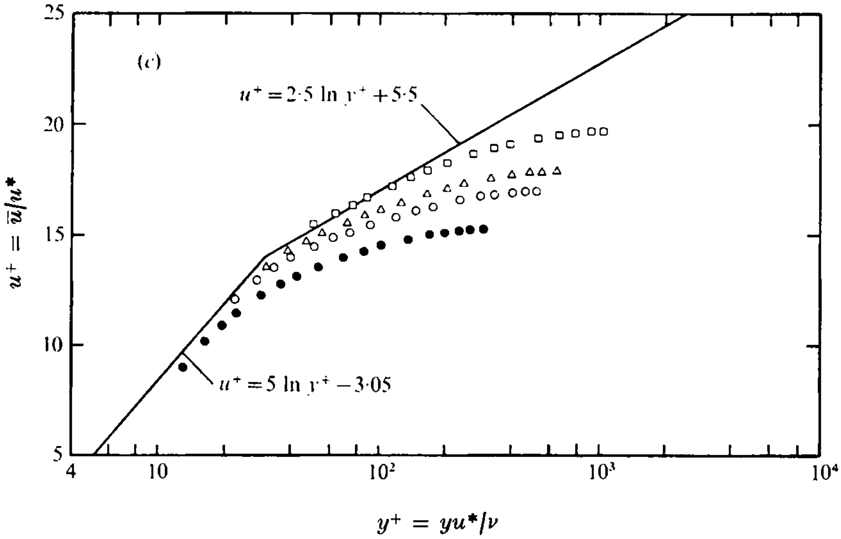

FIGURE 10. Experimental dimensionless velocity profiles in inner zone. (a) $\alpha = 0{\cdot}1$. (b) $\alpha = 0{\cdot}04$. (c) $\alpha = 0{\cdot}02$.

	○	●	△	□	
(a) $Re \times 10^{-4}$	5·08	7·53	8·82	19·43	
	○	●	△	▲	□
(b) $Re \times 10^{-4}$	2·08	4·00	6·96	10·33	21·62
	●	○	△	□	
(c) $Re \times 10^{-4}$	4·05	7·89	11·70	20·93	

between the experimental data and the calculations by Quarmby (1968*b*) only amount to about 7–8%. The experimental data and theoretical results show optimum agreement for the regions close to the wall and zero shear stress. In the region in between, the experimental data are higher than the profiles calculated by Quarmby.

Patel (1973) recently published velocity profiles calculated using an advanced 'mixing-length' model taking into account effects on the velocity profile of pressure gradients and wall curvature. Patel showed that his calculations are in good agreement with published experimental results in boundary layers and in the inner zone of annuli for a dimensionless radius of curvature

$$a^* > 28 \quad (a^* = r \times u^*/\nu).$$

An exact comparison of the new measured data with the calculated profiles of Patel is not possible because the relevant computer programs are lacking. However, since the pressure gradients were low in the experiments the results can be compared with the calculated values for a thick boundary layer on a cylinder. For $\alpha = 0{\cdot}02$, figure 15 shows that the calculated values are about 10% lower than the experimental data, indicating that theory and measurements do not agree for $a^* > 28$, too. If the pressure gradient had been considered the calculated profile would tend to even lower values.

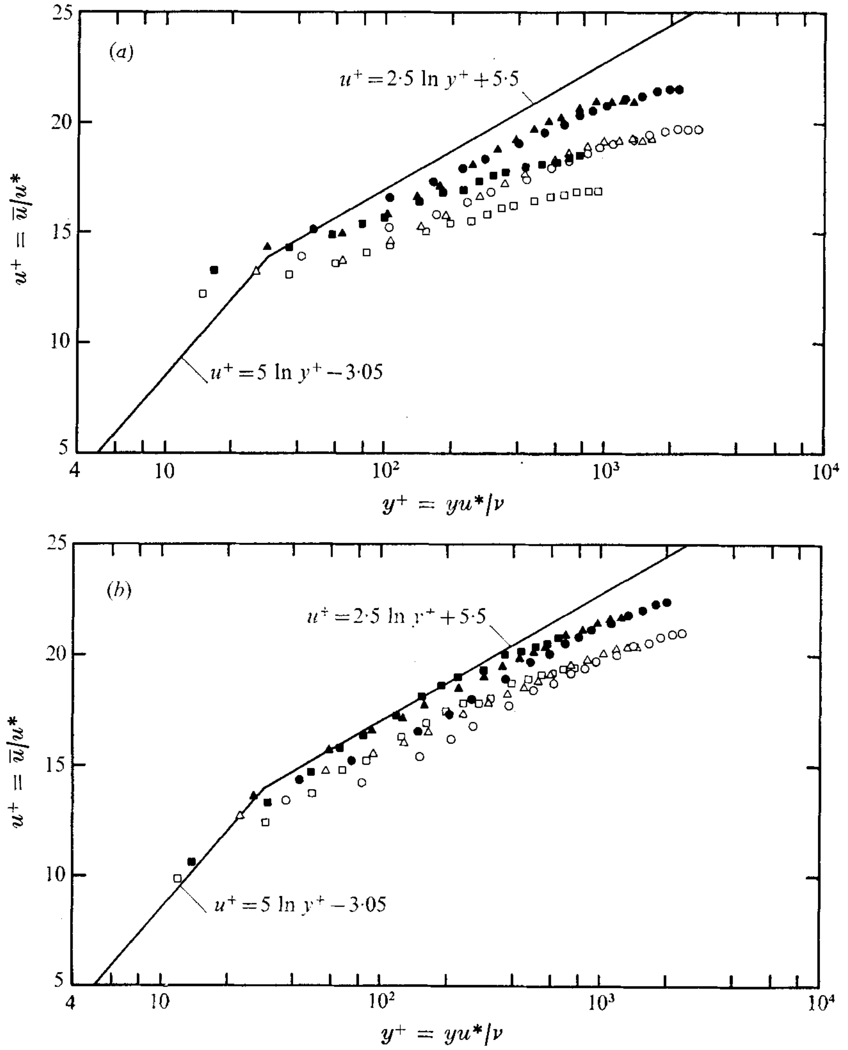

FIGURE 11. Experimental results of Brighton for the inner zone: original (open symbols) and shifted data (solid symbols). (*a*) $\alpha = 0{\cdot}0625$. □, $Re = 0{\cdot}958 \times 10^5$; △, $Re = 1{\cdot}94 \times 10^5$; ○, $Re = 3{\cdot}27 \times 10^5$. (*b*) $\alpha = 0{\cdot}125$. □, $Re = 0{\cdot}89 \times 10^5$; △, $Re = 1{\cdot}82 \times 10^5$; ○, $Re = 3{\cdot}08 \times 10^5$.

It is supposed that the velocity profile of the inner zone of the flow through concentric annuli not only is being affected by the pressure gradient and the curvature of the wall but also, especially in the region near the zero-shear-stress line, by the flow phenomena in the outer zone of the annulus.

4. Conclusions

In summary, it can be said that this investigation has confirmed some theoretical work in the literature with respect to the pressure-drop coefficients of annuli and their dependence on the radius ratio. The non-coincidence between

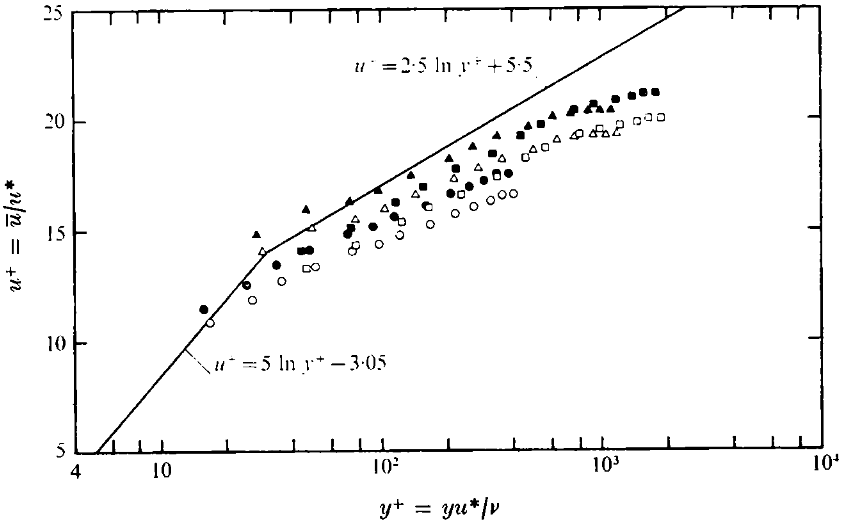

FIGURE 12. Experimental results of Lawn & Elliott for the inner zone: original (open symbols) and shifted data (solid symbols). $\alpha = 0{\cdot}088$. ○, $Re = 3{\cdot}62 \times 10^4$; △, $Re = 12{\cdot}00 \times 10^4$; □, $Re = 20{\cdot}10 \times 10^4$.

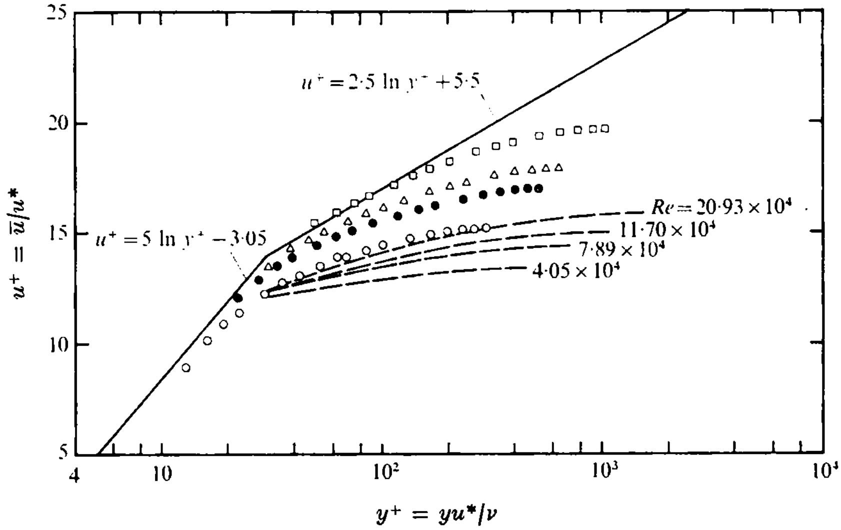

FIGURE 13. Present experimental results and predictions of Eifler for the inner zone. $\alpha = 0{\cdot}02$. ○, $Re = 4{\cdot}05 \times 10^4$; ●, $Re = 7{\cdot}89 \times 10^4$; △, $Re = 11{\cdot}70 \times 10^4$; □, $Re = 20{\cdot}93 \times 10^4$; – – –, theory.

zero shear stress and maximum velocity, which had been assumed and measured in a few experiments, was clearly proved. Moreover, the experimental results showed that the velocity and turbulence distributions are greatly disturbed by the spacers or by the sag of the core rods and wires, respectively, in the case of horizontal test sections. These disturbances affect in particular the position of zero shear stress (or maximum velocity), which is most important for the determination of the flow parameters.

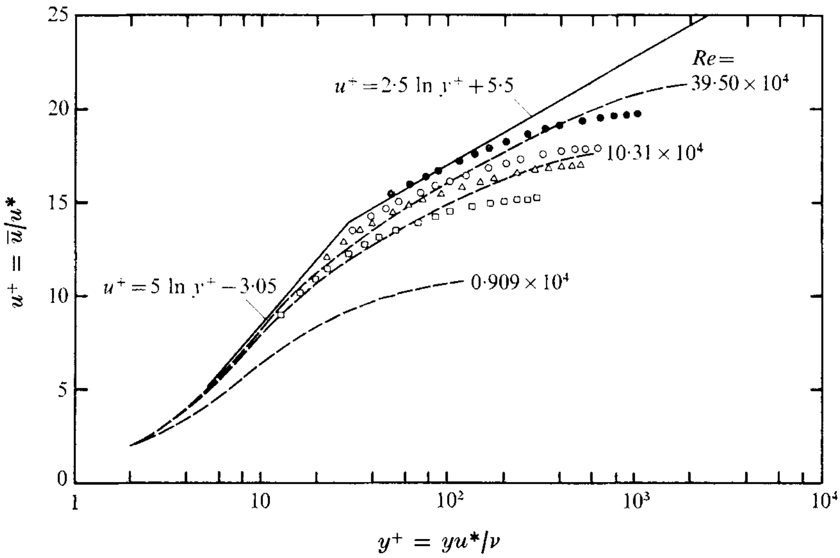

FIGURE 14. Present experimental results and predictions of Quarmby for the inner zone. $\alpha = 0{\cdot}02$. □, $Re = 4{\cdot}05 \times 10^4$; △, $Re = 7{\cdot}89 \times 10^4$; ○, $Re = 11{\cdot}70 \times 10^4$; ●, $Re = 20{\cdot}93 \times 10^4$; – – –, theory.

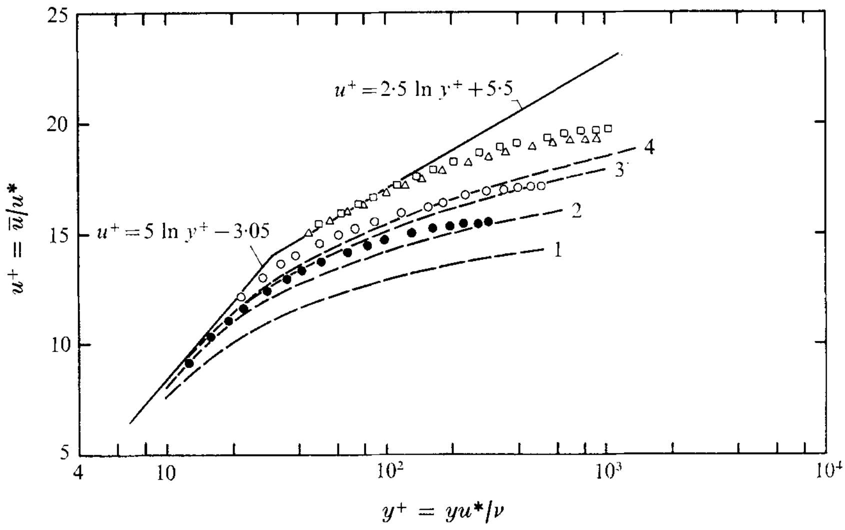

FIGURE 15. Present experimental results and predictions of Patel for the inner zone. $\alpha = 0{\cdot}02$. 1, ●, $Re = 4{\cdot}07 \times 10^4$, $a^* = 32{\cdot}6$; 2, ○, $Re = 7{\cdot}91 \times 10^4$, $a^* = 56{\cdot}5$; 3, △, $Re = 18{\cdot}31 \times 10^4$, $a^* = 101$; 4, □, $Re = 20{\cdot}99 \times 10^4$, $a^* = 137$; – – –, theory.

The new and more precise experimental results with respect to the position of zero shear stress have established also the main cause of the great deviations of the velocity profiles in the inner zone of annuli from the velocity profiles in circular tubes. These deviations, especially in the experimental results by Brighton, have met with general approval in the literature. The large number of models developed to calculate the flow through annuli on the basis of Brighton's results are not in agreement with reality. The theoretical analysis whose results agree perhaps best with the experimental data proved to be the analysis by Quarmby (1968*b*); his calculations start from the circular-tube laws. Quarmby's results fit the experimental positions of zero shear stress quite well, especially the dependence of this position on the Reynolds number. Moreover, the calculated and experimental velocity profiles show optimum agreement.

At the sufficiently high Reynolds numbers assumed, the methods based on the laws of the wall (Maubach 1970) and used to interpret measurements in annuli (Maubach 1972) and rod bundles (Maubach & Rehme 1973) with artificial surface roughnesses are sufficiently well suited for calculations of the flow parameters in smooth annuli also. This is understandable, because the law of the wall of Nikuradse stems from the fact that the influence of the Reynolds number on the velocity profile is neglected, which results in a law for the velocity distribution which is slightly on the crude side.

The theoretical models allowing for the deviations of the velocity profile from the law of the wall, which were elaborated by fitting Brighton's experimental results to annuli, were used and are at present being used for other geometries, especially for rod bundles. Calculations with these models result in deviations of the pressure-drop coefficients. The consequences of the new results have been discussed already for rod bundles in hexagonal (Rehme 1972*b*) and square arrays (Marek, Maubach & Rehme 1973).

The minor effect of geometry on the velocity profile, which was demonstrated by this investigation, and therefore the rather good correlation of the velocity profiles with the law of the wall of course are the reasons for the excellent agreement between calculated and measured pressure-drop coefficients of turbulent flow through different non-circular channels (Rehme 1973).

The author wishes to express his gratitude to Mr E. Mensinger and Mr G. Wörner for their invaluable help with the construction of the test rig, the performance of the experiments and the evaluation of the results.

REFERENCES

BALL, H. D. & AZER, N. Z. 1972 Experimental investigations of eddy diffusivities of air in turbulent annular flow. *Proc. 1972 Heat Transfer & Fluid Mech. Inst., San Fernando Valley*, p. 19. Stanford University Press.

BARROW, H., LEE, Y. & ROBERTS, A. 1965 The similarity hypothesis applied to turbulent flow in an annulus. *Int. J. Heat Mass Transfer*, **8**, 1499.

BARTHELS, H. 1967 Darstellung des Wärmeübergangs in konzentrischen Ringspalten unter Benutzung der Analogie zwischen Impuls- und Wärmeaustausch. *K.F.A. Jülich Rep.* Jül-506-RB.

BRIGHTON, J. A. 1963 The structure of fully developed turbulent flow in annuli. Ph.D. thesis, Purdue University.

BRIGHTON, J. A. & JONES, J. B. 1964 Fully developed turbulent flow in annuli. *J. Basic Engng*, D **86**, 835.

CLUMP, C. W. & KWASNOSKI, D. 1968 Turbulent flow in concentric annuli. *A.I.Ch.E. J.* **14**, 164.

CROOKSTON, R. B. 1966 Heat and momentum transfer for turbulent flow in annuli with small cores. Ph.D. thesis, Carnegie Institute of Technology, Pittsburgh.

CROOKSTON, R. B., ROTHFUS, R. R. & KERMODE, R. I. 1968 Turbulent heat transfer in annuli with small cores. *Int. J. Heat Mass Transfer*, **11**, 415.

DAVIS, E. S. 1943 Heat transfer and pressure drop in annuli. *Trans. A.S.M.E.* **65**, 755.

DEISSLER, R. G. 1955 Analysis of turbulent heat transfer, mass transfer and fluid friction in smooth tubes at high Prandtl and Schmidt numbers. *N.A.C.A. Rep.* no. 1210.

DURST, F., MELLING, A. & WHITELAW, J. H. 1971 The interpretation of hot wire signals in low turbulence flows, *Imperial College Rep.* ET/TN/B/5.

EIFLER, W. 1968 Über die turbulente Geschwindigkeitsverteilung und Wandreibung in Strömungskanälen verschiedener Querschnitte. Ph.D. dissertation, Technische Hochschule, Darmstadt.

EIFLER, W. 1969 Berechnung der turbulenten Geschwindigkeitsverteilung und der Wandreibung in konzentrischen Ringspalten. *Wärme- & Stoffübertragung*, **2**, 36.

EIFLER, W. 1970 Begrenzungen für die Anwendbarkeit von Preston-Rohren in Kanalströmungen. *Wärme- & Stoffübertragung*, **3**, 58.

GOLDSTEIN, S. 1938 *Modern Developments in Fluid Dynamics*, vol. 2, p. 331. Oxford University Press.

GRÄBER, H. 1970 Der Wärmeübergang in glatten Rohren, zwischen parallelen Platten, in Ringspalten und längs Rohrbündeln bei exponentieller Wärmeflußverteilung in erzwungener laminarer oder turbulenter Strömung, *Int. J. Heat Mass Transfer*, **13**, 1645.

IVEY, C. M. 1965 The position of maximum velocity in annular flow. MSc thesis, University of Windsor, Canada.

JONSSON, V. K. 1965 Experimental studies of turbulent flow phenomena in eccentric annuli. Ph.D. thesis, University of Minnesota, Minneapolis.

JONSSON, V. K. & SPARROW, E. M. 1966 Experiments on turbulent-flow phenomena in eccentric annular ducts. *J. Fluid Mech.* **25**, 65.

KAYS, W. M. & LEUNG, E. Y. 1963 Heat transfer in annular passages – hydrodynamically developed turbulent flow with arbitrarily prescribed heat flux. *Int. J. Heat Mass Transfer*, **6**, 537.

KJELLSTRÖM, B. & HEDBERG, S. 1966 On shear stress distributions for flow in smooth or partially rough annuli. *AB Atomenergi, Stockholm Rep.* AE-243.

KJELLSTRÖM, B. & HEDBERG, S. 1968 Calibration experiments with a DISA hot-wire anemometer. *AB Atomenergi, Stockholm, Rep.* AE-338.

KJELLSTRÖM, B. & HEDBERG, S. 1970 Die Eichung eines DISA Hitzdrahtanemometers und Bestätigung der Eichung durch Messungen in einem zylindrischen Kanal. *DISA Inf.* **9**, 8.

KNUDSEN, J. G. & KATZ, D. L. 1950 Velocity profiles in annuli. *Proc. Midwest. Conf. Fluid Dynamics, 1st Conf. Univ. Illinois, Ann Arbor*, p. 175.

KNUDSEN, J. G. & KATZ, D. L. 1958 *Fluid Dynamics and Heat Transfer*. McGraw-Hill.

KOCH, R. & FEIND, K. 1958 Druckverlust und Wärmeübergang in Ringspalten. *Chem.-Ing.-Tech.* **30**, 577.

LAUFER, J. 1954 The structure of turbulence in fully developed pipe flow. *N.A.C.A. Tech. Note*, no. 1174.

LAWN, C. J. & ELLIOTT, C. J. 1971 Fully developed turbulent flow through concentric annuli. *C.E.G.B. Rep.* RD/B/N 1878.

LAWN, C. J. & ELLIOTT, C. J. 1972 Fully developed turbulent flow through concentric annuli. *J. Mech. Eng. Sci.* **14**, 195.

LEE, J. 1965 On von Kármán's eddy viscosity in bounded flow. *Appl. Sci. Res.* A **14**, 250.

LEE, Y. 1964 Turbulent flow and heat transfer in concentric and eccentric annuli. Ph.D. thesis, University of Liverpool.

LEUNG, E. Y., KAYS, W. M. & REYNOLDS, W. C. 1962 Heat transfer with turbulent flow in concentric and eccentric annuli with constant and variable heat flux. *Stanford Rep.* AHT-4.

LEVY, S. 1967 Turbulent flow in an annulus. *J. Heat Transfer*, **89**, 25.

LORENZ, F. R. 1932 Über turbulente Strömung durch Rohre mit kreisringförmigem Querschnitt. *Mitt. Inst. Strömungsmaschinen, TH Karlsruhe*, no. 2.

MACAGNO, E. O. & MCDOUGALL, D. W. 1966 Turbulent flow in annular pipes. *A.I.Ch.E. J.* **12**, 437.

MACMILLAN, F. A. 1956 Experiments on Pitot-tubes in shear flow. *Aero. Res. Counc. R. & M.* no. 3028.

MAREK, J., MAUBACH, K. & REHME, K. 1973 Heat transfer and pressure drop performance of rod bundles arranged in square arrays. *Int. J. Heat Mass Transfer*, **16**, 2215.

MAUBACH, K. 1969 Reibungsgesetze turbulenter Strömungen in geschlossenen, glatten und rauhen Kanälen von beliebigem Querschnitt. Ph.D. dissertation. University of Karlsruhe. (*Kernforschungszentrum Karlsruhe Ext. Rep.* INR-4/69-22.)

MAUBACH, K. 1970 Reibungsgesetze turbulenter Strömungen. *Chem.-Ing.-Tech.* **42**, 995.

MAUBACH, K. 1972 Rough annulus pressure-drop: interpretation of experiments and recalculation for square ribs. *Int. J. Heat Mass Transfer*, **15**, 2489.

MAUBACH, K. & REHME, K. 1972 Negative eddy diffusivities for asymmetric turbulent velocity profiles? *Int. J. Heat Mass Transfer*, **15**, 425.

MAUBACH, K. & REHME, K. 1973 Pressure drop for parallel flow through a roughened rod cluster. *Nucl. Engng Design*, **25**, 369.

MICHIYOSHI, I. & NAKAJIMA, T. 1968 Fully developed turbulent flow in a concentric annulus. *J. Nucl. Sci. Tech.* **5**, 354.

MIN, T. C., HOFFMAN, H. W. & PEEBLES, F. N. 1971 A bilateral approach to the analysis of turbulent flow in an annulus. *Nucl. Engng Design*, **15**, 65.

NICOL, A. A. & MEDWELL, J. O. 1964 Velocity profiles and roughness effects in annular pipes. *J. Mech. Engng Sci.* **6**, 110.

NIKURADSE, J. 1932 Gesetzmäßigkeiten der turbulenten Strömung in glatten Rohren. *Forsch.-Arb. Geb. Ing.-Wes., VDI-Forschungsheft*, no. 356.

OKIISHI, T. H. & SEROVY, G. K. 1964 Experimental velocity profiles for fully developed turbulent flow of air in concentric annuli. *A.S.M.E. Paper*, 64-WA/FE-32 (1964).

PATEL, V. C. 1965 Calibration of the Preston tube and limitation on its use in pressure gradients. *J. Fluid Mech.* **23**, 185.

PATEL, V. C. 1973 A unified view of the law of the wall using mixing-length theory. *Aero. Quart.* **24**, 55.

PRESTON, J. H. 1954 The determination of turbulent skin friction by means of Pitot tubes. *J. Roy. Aero. Soc.* **58**, 109.

QUARMBY, A. 1967*a* On the use of the Preston tube in concentric annuli. *Aeron. J. Roy. Aero. Soc.* **71**, 47.

QUARMBY, A. 1967*b* An experimental study of turbulent flow through concentric annuli. *Int. J. Mech. Sci.* **9**, 205.

QUARMBY, A. 1968*a* The ratio of the wall shear stresses in concentric annuli. *Aeron. J. Roy. Aero. Soc.* **72**, 345.

QUARMBY, A. 1968*b* An analysis of turbulent flow in concentric annuli. *Appl. Sci. Res.* **19**, 250.

QUARMBY, A. 1969 Improved application of the von Kármán similarity hypothesis to turbulent flow in ducts. *J. Mech. Engng Sci.* **11**, 14.

QUARMBY, A. & ANAND, R. K. 1970 Turbulent heat transfer in concentric annuli with constant wall temperatures. *J. Heat Transfer*, **92**, 33.

RAO, G. N. V. & KESHAVAN, N. R. 1972 Axisymmetric boundary layers in zero pressure-gradient flows. *J. Appl. Mech.* **39**, 25.

RATKOWSKY, D. A. 1966 Fluid friction and heat transfer in plain, concentric annuli. *Can. J. Chem. Engng*, **44**, 8.

REHME, K. 1972*a* Untersuchungen der Turbulenz- und Schubspannungsverteilung an einem Kreisrohr mit einem Hitzdraht-Anemometer. *Kernforschungszentrum Karlsruhe Rep.* KFK 1642.

REHME, K. 1972*b* Pressure drop performance of rod bundles in hexagonal arrangements. *Int. J. Heat Mass Transfer*, **15**, 2499.

REHME, K. 1973 Simple method of predicting friction factors of turbulent flow in non-circular channels. *Int. J. Heat Mass Transfer*, **16**, 933.

ROBERTS, A. 1967 A comment on the turbulent flow velocity profile in a concentric annulus. *Int. J. Heat Mass Transfer*, **10**, 709.

ROTHFUS, R. R. 1948 Velocity gradients and friction in concentric annuli. Ph.D. thesis, Carnegie Institute of Technology.

ROTHFUS, R. R., MONRAD, C. C. & SENECAL, K. E. 1950 Velocity distribution and fluid friction in smooth concentric annuli. *Ind. Engng Chem.* **42**, 2511.

ROTHFUS, R. R., MONRAD, C. C., SIKCHI, K. G. & HEIDEGER, W. J. 1955 Isothermal skin friction in flow through annular sections. *Ind. Engng Chem.* **47**, 913.

ROTHFUS, R. R., SARTORY, W. K. & KERMODE, R. I. 1966 Flow in concentric annuli at high Reynolds numbers. *A.I.Ch.E. J.* **12**, 1086.

ROTHFUS, R. R., WALKER, J. E. & WHAN, G. A. 1958 Correlation of local velocities in tubes, annuli, and parallel plates. *A.I.Ch.E. J.* **4**, 240.

SARTORY, W. K. 1962 Turbulent flow in annular ducts. Ph.D. thesis, Carnegie Institute of Technology, Pittsburgh.

SMITH, S. L., LAWN, C. J. & HAMLIN, M. J. 1968 The direct measurement of wall shear stress in an annulus. *C.E.G.B. Rep.* RD/B/N 1232.

TIEDT, W. 1966 Bereehnung des laminaren und turbulenten Reibungswiderstandes konzentrischer und exzentrischer Ringspalte. *Chem.-Ztg./Chem. Appl.* **90**, 813.

TIEDT, W. 1967 Berechnung des laminaren und turbulenten Reibungswiderstandes konzentrischer und exzentrischer Ringspalte. *Chem.-Ztg./Chem. Appl.* **91**, 17, 149, 299, 569, 968.

TIEDT, W. 1968 Berschnung des laminaren und turbulenten Reibungswiderstandes konzentrischer und exzentrischer Ringspalte. *Chem.-Ztg./Chem. Appl.* **92**, 76.

WILSON, N. W. & MEDWELL, J. O. 1968 An analysis of heat transfer for fully developed turbulent flow in concentric annuli. *J. Heat Transfer*, **90**, 43.